JOURNAL OF COMPUTATIONAL PHYSICS 48, 246–269 (1982)

Influence of Boundary Approximations and Conditions on Finite-Difference Solutions*

F. G. BLOTTNER

Sandia National Laboratories, Albuquerque, New Mexico 87185

Received January 6, 1982

Numerical representations of boundary approximations and conditions for three problems are investigated to determine the resulting global accuracy of the steady-state solution. Numerical accuracy with various boundary approximations is determined for quasi-one-dimensional inviscid flow in a duct with the interior grid points evaluated using the MacCormack scheme. When an extrapolation approximation with first-order local truncation error is used, the global second-order accuracy of the difference scheme can be destroyed. For one-dimensional flow in a porous medium, an implicit midpoint difference scheme which is consistent with the boundary conditions is developed without the need of boundary approximations. A dissipative model problem is solved with the boundary conditions discretized with first- and second-order accuracy. The overall second-order accuracy of the difference scheme is destroyed if first-order numerical representation of one of the boundary conditions is used. With a boundary approximation, the second-order global accuracy of the model problem is retained if either second-order extrapolation or first-order representation of the governing equation is used.

INTRODUCTION

Finite-difference schemes are usually developed for computing the interior points of the computational domain and then boundary conditions and special relations are used at and near boundaries. For a given set of governing equations, there are appropriate boundary conditions that result in a well-posed problem with continuous solutions and provide relations which allow some of the dependent variables to be determined at the boundaries. These boundary conditions are usually obtained from the physics of the problem. The remaining relations required to determine the dependent variables at the boundaries must be determined from boundary approximations such as extrapolation, characteristic compatibility relations, or difference relations obtained from the governing equations. The boundary approximations can influence the stability of the overall scheme and can influence the global accuracy of the difference approximation. These properties of the boundary approximations must be investigated for each interior difference scheme and set of governing equations. A review of this problem has been given recently by Turkel [1]. Gustafsson [2]

* This work performed at Sandia National Laboratories supported by the U.S. Department of Energy under Contract DE-AC04-76DP00789.

0021-9991/82/110246-24$02.00/0

indicates that boundary approximations for the transient solution of hyperbolic equations can be differenced with one order lower accuracy than used for the interior difference scheme without decreasing the overall accuracy. This statement is perhaps misleading due to the accuracy definition. Skollermo [3] restates this conclusion as "formally, the local truncation error in the boundary approximation should also be of the same order as the global error of the interior scheme." Bramble and Hubbard [4] have shown that the solution of Poisson's equation with Dirichlet boundary conditions on an irregular computational region can use first-order difference relations of the governing equation near the boundary and still provide an overall second-order scheme. In this case the boundary condition can be satisfied exactly but the governing equation has a local truncation error of order of the step size near the boundary due to nonuniform grid spacing. If the solution is interpreted in terms of a uniform grid with grid points exterior to the boundary, the boundary condition discretization uses quadratic extrapolation for the exterior grid points. Thomas [5] investigated the boundary approximations with implicit ADI techniques at various flow boundaries that occur in external and internal flow problems. The boundary approximations are conservatively differenced forms of the flow equations and have a local truncation error that is first order. The global truncation error in space is indicated to be second-order accurate but no numerical results are given to demonstrate this behavior.

The present study is concerned with obtaining a better understanding of the influence numerical representations of the boundary approximations and conditions have on the global accuracy of the finite-difference solution to steady-state problems. Quasi-one-dimensional flow in a duct is used as an illustration of the influence boundary approximations have on the global accuracy when the MacCormack explicit scheme is used for the interior grid points. The steady-state problem is obtained from the asymptotic time solution of the transient equations. The case of subsonic entry to supersonic exit flow has previously been investigated by Turkel [1] while the present study is concerned with this problem plus the case of complete subsonic flow where an exit boundary condition must be specified. The numerical treatment of computational boundaries for a limited region with subsonic flow is discussed by Moretti and Pandolfi [6]. A physical model of the flow outside of the boundaries provides the boundary conditions which can interact with the interior flow.

The importance of the interior difference scheme is illustrated with the problem of compressible flow through a porous material where the governing equations are the same as the quasi-one-dimensional problem with a friction term added. The porosity of the material corresponds to the cross-sectional area of the duct, and for low speed flows the friction factor is related to the permeability of the porous material. The problem considered is the steady-state subsonic flow resulting from a pressure drop across the porous material. The solution is obtained with an implicit midpoint difference scheme which provides exactly the correct number of difference relations along with the boundary conditions needed to solve for the dependent variables at all of the grid points. Therefore, with this approach the interior difference relations are

not supplemented with boundary approximations. With central differences, three boundary or extraneous approximations are required for this problem and the influence on the global error is investigated.

Finally, a dissipative model problem is studied to illustrate the effect of numerical discretization of the boundary conditions and boundary approximations on global error. For this case the global error is determined both numerically and analytically.

Quasi-One-Dimensional Flow

The properties of the governing equations for transient flow in a duct are well understood from the point of view of the method of characteristics and are described by Shapiro [7]. This relatively simple flow problem provides an excellent test case for studying the effects of boundary conditions and approximations as the exact steady-state solution for this flow is known. The quasi-one-dimensional flow problem is also of engineering interest to approximate more complex flows. The time-dependent approach is used in the present study to obtain the steady-state continuous solution to the flow in a duct with subsonic entry flow and with either subsonic or supersonic exit flow. The flow in a nozzle with supersonic flow has been investigated by Turkel [1] with both continuous flow and with a shock where a downstream pressure is specified. The handling of computational boundaries for subsonic flows has been investigated by Moretti and Pandolfi [6].

The quasi-one-dimensional inviscid flow equations are written as

$$(\partial Q/\partial t) + (\partial F/\partial x) = S, \tag{1}$$

where

$$Q = \begin{bmatrix} \rho A \\ \rho u A \\ eA \end{bmatrix}, \qquad F = \begin{bmatrix} \rho u A \\ (\rho u^2 + p) A \\ (e + p) uA \end{bmatrix}, \qquad S = \begin{bmatrix} 0 \\ p(dA/dx) \\ 0 \end{bmatrix}.$$

The variable A is the cross-sectional area of the duct and the remaining variables have the usual meaning. The total energy is defined as

$$e = \rho(h + \tfrac{1}{2}u^2) - p, \tag{2}$$

where the enthalpy for a perfect gas is

$$h = (\gamma/(\gamma - 1))\, p/\rho. \tag{3}$$

The characteristics of governing equations (1) are

$$dx/dt = u \pm c \qquad \text{(Mach lines)}, \qquad dx/dt = u \qquad \text{(Path lines)}, \tag{4}$$

where the speed of sound for a perfect gas is determined from $c = \sqrt{\gamma p/\rho}$. The compatibility relations along the characteristics are

$$\rho u\, du \pm dp \pm (pu\gamma/A)(dA/dx)\, dt = 0 \qquad \text{along} \quad u \pm c,$$
$$dp - c^2\, d\rho = 0 \qquad \text{along} \quad u. \tag{5}$$

These relations can be written as finite-difference equations and used to determine the solution at the next time step from the appropriate initial and boundary conditions. A finite-difference approach for solving governing equations (1) is used rather than the method of characteristics. The above relations are given to help understand the physical boundary conditions and to obtain computational relations at the boundaries.

The dependent variables at the interior grid points are advanced in time with the MacCormack explicit scheme. The variables are first predicted at time $(n+1)$ with first-order accuracy from the known conditions at time (n) and then a corrector is used to obtain the new results at time $(n+1)$ with second-order accuracy. The difference relations for governing equations (1) with the backward–forward difference version are

$$\bar{Q}_i = Q_i^n - (\Delta t/\Delta x)(F_i - F_{i-1})^n + \Delta t\, S_{i-1/2}^n, \qquad i = 2, 3, \ldots, I,$$
$$Q_i^{n+1} = \tfrac{1}{2}[Q_i^n + \bar{Q}_i - (\Delta t/\Delta x)(\bar{F}_{i+1} - \bar{F}_i) + \Delta t\, \bar{S}_{i+1/2}], \qquad i = I-1, I-2, \ldots, 2. \tag{6}$$

The MacCormack scheme requires the following Courant number restriction:

$$C = (|u| + c)\, \Delta t/\Delta x \leqslant 1. \tag{7}$$

When the steady-state solution is obtained with the MacCormack scheme, governing equations (1) are effectively evaluated with a midpoint difference scheme, which is second-order accurate in space.

At the boundaries of the computational domain the MacCormack difference relations are not adequate and additional difference relations must be used along with the boundary conditions to complete the solution procedure for $\bar{Q}_1$ and Q_I^{n+1}. In addition, the variations of three dependent variables along the duct at the initial time is also required to start the solution.

For the case of subsonic entry flow, the $u + c$ and u characteristics are entering the computational domain and the $u - c$ characteristic is leaving the computational domain. Therefore, two conditions must be specified and the remaining dependent variable must be determined from the compatibility relation of Eq. (5) along the $u - c$ characteristic or from some other difference relation. Since in the present study only the steady-state solution is desired, the two physical boundary conditions utilize the steady-state isentropic relations for the entry pressure and density as a function of the entry Mach number, stagnation density, and stagnation pressure

$$\rho_1 = \rho_0(1 + \tfrac{1}{2}(\gamma - 1)\, M_1^2)^{-1/(\gamma-1)}, \qquad p_1 = p_0(\rho_1/\rho_0)^{\gamma}, \tag{8}$$

where

$$M_1^2 = u_1^2/(\gamma - \tfrac{1}{2}(\gamma - 1)\, u_1^2)$$

The subscript 1 indicates the entry conditions while subscript 0 indicates the variables are stagnation conditions in an infinite reservoir. The above relations assume quasi-steady streamtube flow to determine the pressure and density from the entry velocity and become exact for the steady-state solution. For steady-state conditions, governing equations (1) are evaluated with a midpoint scheme where subscript 1 and 2 are the entry point and next grid point downstream. The three difference relations involve the quantities ρ, u, p, and e at the grid points 1 and 2. These variables are unknown at grid point 1 and known at grid points 2 from the interior difference scheme. The system of equations is completed with total energy relations (2) and equation of state (3). These relations are used to solve for the entry velocity at the new time level after the corrector step of the MacCormack difference scheme has been used to determine the dependent variables at grid point 2.

$$u_1 = (-b + \sqrt{b^2 - 4ac})/2a, \tag{9}$$

where

$$a = 1 - (4\gamma/(\gamma - 1))\, A_1/(A_1 + A_2),$$
$$b = (1 - a)[(\rho u^2 A)_2 + \tfrac{1}{2} p_2 (A_1 + A_2)]/(\rho u A)_2,$$
$$c = -2[(e + p)/\rho]_2.$$

Equation (9) is second-order accurate and consistent with the MacCormack scheme when the steady-state solution is obtained and replaces the compatibility relation, Eq. (5). An extrapolation technique is often used to obtain a dependent variable at the boundary if a physical boundary condition does not specify the variable. The following linear extrapolation relation for the velocity at the entry has been investigated:

$$u_1 = 2u_2 - u_3, \tag{10}$$

where the velocities are at the $(n + 1)$ time level.

For subsonic exit flow, there are two characteristics leaving the computational domain and one entering. For supersonic flow, all three characteristics leave the computational domain. Therefore, one physical boundary condition is required for subsonic flow at the exit while no boundary conditions can be specified for continuous supersonic exit flow. Three boundary relations have been investigated for subsonic exit flow and are applied to obtain the dependent variables at the $(n + 1)$ time level.

The *characteristic boundary relation* method uses the compatibility conditions,

Eq. (5), along the $u + c$ and u characteristics to obtain the first-order finite-difference relations

$$u_I^{n+1} = u_a - [\, p_I^{n+1} - p_a + ((pu\gamma/A)(dA/dx))_I \, \Delta t]/(\rho c)_I, \tag{11a}$$

$$\rho_I^{n+1} = \rho_b + (p_I^{n+1} - p_b)/c_I^2. \tag{11b}$$

For subsonic flow the exit pressure p_I^{n+1} is specified. The dependent variables at the grid points a and b are at time n and are on the $u + c$ and u characteristics, respectively. Linear interpolation along with a first-order difference relation for the characteristic locations are used to determine these variables as follows:

$$W_a = (1 - \alpha)\, W_I + \alpha\, W_{I-1}, \qquad \text{where} \quad W = u \quad \text{or} \quad p,$$

$$W_b = (1 - \beta)\, W_I + \beta\, W_{I-1}, \qquad \text{where} \quad W = p \quad \text{or} \quad \rho, \tag{12}$$

and the coefficients are

$$\alpha = \Delta t(u_I + c_I)/\Delta x, \qquad \beta = \Delta t\, u_I/\Delta x.$$

With the above relations and Eq. (12) used in Eqs. (11), the right sides of these equations are known and the exit velocity and density can be determined.

The *unsteady midpoint boundary relations* are developed from continuity and momentum equations (1) using one-sided spatial differences and are written in the following finite-difference form:

$$((Q^{n+1} - Q^n)/\Delta t)_I + ((F_I - F_{I-1})/\Delta x)^{n+1} = \tfrac{1}{2}(S_I + S_{I-1})^{n+1}. \tag{13}$$

The continuity equation becomes

$$(\rho A)_I^{n+1} = [(\rho A)_I^n + (\Delta t/\Delta x)(\rho u A)_{I-1}^{n+1}]/(1 + (\Delta t/\Delta x)\, u_I^{n+1}). \tag{14}$$

Momentum equation (13) and the above continuity equation (14) are combined to obtain the exit velocity

$$u_I^{n+1} = \{(\rho u A)_I^n + \Delta t[(\rho u^2 A)_{I-1}^{n+1} - \tfrac{1}{2}(p_I - p_{I-1})^{n+1}(A_I + A_{I-1})]/\Delta x\}$$
$$\times \{(\rho A)_I^n + \Delta t(\rho u A)_{I-1}^{n+1}/\Delta x\}^{-1}. \tag{15}$$

With exit velocity determined from Eq. (15), the density is then evaluated from Eq. (14).

The *extrapolation boundary relations* for a uniform grid spacing use the following expressions to determine the exit density and velocity:

$$\text{first order:} \qquad W_I = W_{I-1} + O(\Delta x), \qquad W = \rho \quad \text{or} \quad u; \tag{16a}$$

$$\text{second order:} \qquad W_I = 2W_{I-1} - W_{I-2} + O(\Delta x^2), \qquad W = \rho \quad \text{or} \quad u. \tag{16b}$$

According to Gustafsson's definition [2], Eqs. (16a) and (16b) are zeroth- and first-order accurate boundary approximations, respectively. The extrapolation procedure

can also use characteristic variables for W and the stability and accuracy of the results might be improved.

The flow in ducts with the geometries utilized by Griffin and Anderson [8] are used to illustrate the accuracy of the various boundary conditions. These geometries are of the Laval nozzle type with the throat height above the centerline used as the reference length L. With entry at $x = 0$, the throat at $x = x_T$ and the exit at $x = x_I$, the area variation of the duct is given as

$$\begin{aligned} A &= 1 + (A_1 - 1)[(x_T - x)/x_T]^2 \qquad \text{for} \quad x \leqslant x_T, \\ &= 1 + (A_I - 1)[(x - x_T)/(x_I - x_T)]^2 \qquad \text{for} \quad x > x_T. \end{aligned} \tag{17}$$

The entry area A_1 and the exit area A_I must be specified to complete the description of the duct.

The *first example* is a duct flow with $A_1 = 1.5$, $A_I = 2.0$, $x_I = 40$, and $x_T = 10$ with supersonic flow at the exit without any shock waves. The exact analytical solution for the isentropic flow is used as the initial conditions for the dependent variables along the duct. The numerical solution is obtained with $\Delta x = 1$ and Δt is chosen at each time step such that the maximum Courant number at any grid point is 0.9. The steady state solution to the finite-difference equations is different than the initial conditions due to truncation error and will be the same only when $\Delta x \to 0$. The MacCormack finite-difference technique is used to obtain the steady-state solution for the duct configuration. The approach of the solution towards a steady state is illustrated in Table I where the entry velocity is presented for the midpoint boundary relation, Eq. (9). With the number of decimal places shown in this table, a steady state is obtained after 400 time steps for the midpoint boundary relation. The time shown is the nondimensional time $(t/L)\sqrt{\rho_0/p_0}$. The result of using the linear extrapolution relation of Eq. (10) for the entry velocity is shown in Table I. After

TABLE I

Entry Velocity for Supersonic Duct

Number of time steps	Time	Midpoint	Extrapolation
0	0	0.499922	0.499922
100	33.5	0.500244	0.498947
200	66.9	0.500247	0.498998
300	100.4	0.500246	0.499271
400	133.9	0.500247	0.499201
500	167.3	0.500247	0.499042
600	200.8	0.500247	0.498816
700	234.3	0.500247	0.498532
800	267.7	0.500247	0.498189
900	301.2	0.500247	0.497781
1000	334.7	0.500247	0.497306

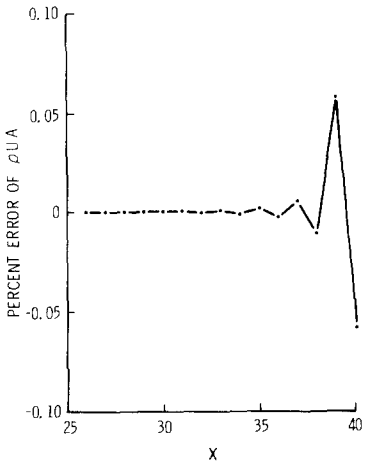

FIG. 1. Infection of computational boundary relation with linear extrapolation and supersonic exit flow.

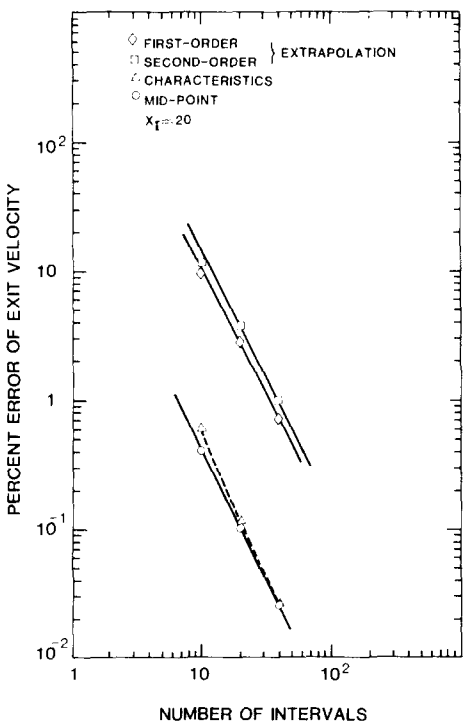

FIG. 2. Accuracy of exit velocity with various exit boundary approximations for steady state quasi-one-dimensional flow.

1000 time steps a steady state is not obtained and this technique appears to give a solution that is drifting. When linear extrapolation is used to determine the dependent variables ρ, u, and p at the exit, a steady-state solution is obtained and the entry velocity is the same as that given in Table I with the midpoint relation, Eq. (9). Since the linear extrapolation relations are not consistent with the MacCormack finite-difference relations, however, the mass flux near the exit oscillates about the "correct" numerical value as shown in Fig. 1. The correct upstream numerical solution is used to judge the error of ρuA and this "correct" numerical solution has an error of 0.053% relative to the exact analytical solution. Although the oscillation shown in Fig. 1 is unpleasant, the error is about the same or less than the truncation error of the "correct" numerical solution with $\Delta x = 1$.

The *second example* considered is subsonic duct flow with $A_1 = 6$, $A_t = 1$, $x_t = 20$, and $x_T = 20$. The pressure at the exit has a value of $0.93716250\, p_0$ and is held fixed as the known physical boundary condition. Steady-state solutions are obtained with $\Delta x = 2$, 1, and 0.5 with 1000, 2000, and 4000 time steps, respectively. The exit velocity is used to judge the spatial accuracy of the steady-state solutions where the exact value of the exit velocity is $0.358610\sqrt{\rho_0/p_0}$. The percent error of the steady-state exit velocity is given in Fig. 2 for the boundary relations given by characteristic

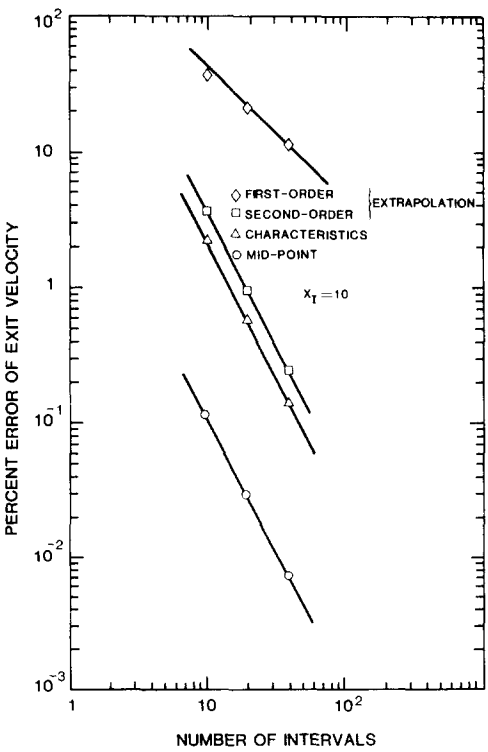

FIG. 3. Accuracy of exit velocity with various exit boundary approximations for steady state quasi-one-dimensional flow.

equation (11), finite-difference equation (15), and extrapolation equation (16). All of the methods have an error behavior that indicates that the spatial differencing is second order. When the characteristic boundary relation is used, the mass flux wiggles at the grid points near the exit with behavior similar to that shown in Fig. 1.

The global second-order behavior with the first-order extrapolation boundary approximation cannot in general be expected to occur. The foregoing example has zero gradients of the dependent variables at the exit and the first-order extrapolation is appropriate. The solution was obtained for the same problem except the exit conditions are applied at $x_f = 10$, where the dependent variable gradients are nonzero. The results of this accuracy study are given in Fig. 3, where the first-order extrapolation boundary approximation results in first-order global accuracy. The other boundary approximations result in global second-order accuracy. The characteristic approximation is based on first-order approximations to the governing equations and does not destroy the global second-order behavior. A boundary approximation which uses the governing equations can have a local truncation error of first order while extrapolation techniques must be second order in order to avoid reduction of the global accuracy.

Flow in Porous Media

One-dimensional high-speed subsonic compressible flow through a porous material is considered. The gas and porous material are allowed to have different temperatures but energy transport due to conduction and dispersion is neglected. The governing equations are of the same form as Eqs. (1) except there are four dependent variables as follows and the flux vector is:

$$Q = \begin{bmatrix} \rho\varepsilon \\ \rho u\varepsilon \\ e_f\varepsilon \\ e_s(1-\varepsilon) \end{bmatrix} = \begin{bmatrix} Q_1 \\ Q_2 \\ Q_3 \\ Q_4 \end{bmatrix}, \qquad F = \begin{bmatrix} \rho u\varepsilon \\ (\rho u^2 + p)\,\varepsilon \\ (e_f + p)\,u\varepsilon \\ 0 \end{bmatrix}, \tag{18}$$

where

ρ = density of fluid,

p = pressure of fluid,

u = local or interstitial velocity of fluid,

e_f = total fluid energy per unit fluid volume,

e_s = total solid energy per unit solid volume $= \rho_s c_s T_s$,

ε = porosity of solid material.

These relations are the same as quasi-one-dimensional equation (1) except the cross-sectional area is replaced by the porosity. The source term in Eq. (1) becomes

$$S = \begin{bmatrix} 0 \\ p(d\varepsilon/dx) - (\alpha\mu + \beta\rho u\varepsilon)\,\varepsilon^2 u \\ -ha_p(T - T_s) \\ ha_p(T - T_s) \end{bmatrix}, \tag{19}$$

where α and β are dependent on the flow resistance model,

h = heat transfer coefficient,

a_p = particle surface area per unit volume of porous media,

$= 6(1 - \varepsilon)/d_p$ for spherical particles of diameter d_p,

T = temperature of fluid $= \bar{M}\varepsilon p/R\rho$,

T_s = temperature of solid porous material.

The coefficients α and β are determined from the Ergun [9] equation for gas flow thru a packed bed of particles with effective diameter d_p

$$\alpha = 150(1 - \varepsilon)^2/(\varepsilon^3 d_p^2), \qquad \beta = 1.75(1 - \varepsilon)/(\varepsilon^3 d_p). \tag{20}$$

The foregoing momentum equation includes the usual Forchheimer equation which relates the pressure gradient to the flow resistance terms. In addition, the momentum equation includes the inertia term as suggested by Emanuel and Jones [10] and predicts choked flow if there is sufficient pressure drop. The energy equations are the Schumann [11] model for heat transfer in a bed of particles except the kinetic energy of the fluid and the work done on the fluid by pressure forces are included.

For subsonic flow everywhere, the governing equations require two boundary conditions at the inflow locations ($x = 0$) and one boundary condition is needed at the outflow ($x = L$). The pressures p_{in} and p_{out} are assumed known at both locations while the gas temperature T_{in} is specified at the inflow. The initial variation of the dependent variables across the porous material is obtained from the steady state isothermal solution with the inertia term neglected in the momentum equation. The pressure variation has been determined by Morrison [12] and the result is

$$p = [\,p_{in}^2 + (p_{out}^2 - p_{in}^2)(x/L)\,]^{1/2}. \tag{21}$$

The mass flux density is

$$\rho u\varepsilon = \{-\alpha\mu + [(\alpha\mu)^2 + 2\beta(p_{in}^2 - p_{out}^2)\,\rho/pL\,]^{1/2}\}/2\beta. \tag{22}$$

The density is determined from the equation of state with the inflow temperature used along with the pressure obtained from Eq. (21).

This investigation is concerned with obtaining the steady-state solution where the solid and gas temperatures are the same at any location without heat transfer between the two phases. The adiabatic flow case has an exact solution, but for the present formulation a difficult iteration process is required to determine the inflow Mach number. Therefore, even for the steady-state solution, an efficient numerical solution is needed. The initial approach considers the steady-state form of Eq. (1) and uses midpoint difference relations to obtain the difference equations

$$(F_{i+1} - F_i)/\Delta x_i = \tfrac{1}{2}(S_{i+1} + S_i), \tag{23}$$

where $\Delta x_i = x_{i+1} - x_i$. The quantities F and S are linearized about the previous known value which is indicated with a bar and the expansions are

$$F = \bar{F} + \tilde{A}\Delta Q + \cdots, \qquad S = \bar{S} + \tilde{D}\Delta Q + \cdots, \tag{24}$$

where $\Delta Q = Q - \bar{Q}$. The Jacobian matrices A and D are obtained from

$$\tilde{A} = \partial F/\partial Q, \qquad \tilde{D} = \partial S/\partial Q.$$

Difference equation (23) becomes

$$\begin{aligned}(\tilde{A}_{i+1} - \tfrac{1}{2}\tilde{D}_{i+1}\Delta x_i)\,\Delta Q_{i+1} - (\tilde{A}_i + \tfrac{1}{2}\tilde{D}_i\,\Delta x_i)\,\Delta Q_i \\ = -\bar{F}_{i+1} + \bar{F}_i + \tfrac{1}{2}\Delta x_i(\bar{S}_{i+1} + \bar{S}_i), \quad i = 1, 2, 3, \ldots, I-1,\end{aligned} \tag{25}$$

and the difference equation for the energy equations for the solid has the special form

$$\sum_{n=1}^{4} \tilde{D}_{4n}\Delta Q_n = \bar{S}_4, \qquad i = 1, 2, \ldots, I. \tag{26}$$

The boundary conditions are:

at $x = 0$:

$$\Delta Q_1 = (Q_1)_{\text{in}} - \bar{Q}_1, \qquad \text{where} \quad (Q_1)_{\text{in}} = \bar{M}\varepsilon p_{\text{in}}/RT_{\text{in}}. \tag{27a}$$

at $x = 0$ or L:

$$\tfrac{1}{2}\bar{u}^2\,\Delta Q_1 - \bar{u}\Delta Q_2 + \Delta Q_3 = \varepsilon p_*/(\gamma - 1) - \bar{Q}_3 + \tfrac{1}{2}\bar{Q}_2^2/\bar{Q}_1, \tag{27b}$$

where p_* is p_{in} or p_{out} at the appropriate boundary.

Difference equations (25) and (26) along with boundary conditions (27) provide $4I$ relations which are used to solve for the $4I$ unknown dependent variables at the I grid points. The difference equations and boundary conditions are written as the following block-tridiagonal system:

$$
\begin{aligned}
B_1 W_1 - C_1 W_2 &= D_1, \\
-A_i W_{i-1} + B_i W_i - C_i W_{i+1} &= D_i, \qquad i = 2, 3, \ldots, I-1, \\
-A_I W_{I-1} + B_I W_I &= D_I,
\end{aligned} \tag{28}
$$

where

$$
W_i = \begin{bmatrix} \Delta Q_1 \\ \Delta Q_2 \\ \Delta Q_3 \\ \Delta Q_4 \end{bmatrix}_i
$$

and the governing relations are used in the following manner for the *midpoint* scheme:

At $i = 1$:

boundary condition equation (27a)
momentum equation (25)
boundary condition equation (27b)
solid energy equation (26) (29a)

At $i = 2, 3, \ldots, I-1$:

continuity equation ($i \to i+1$ in Eq. 25)
momentum equation (25)
fluid energy equation (25)
solid energy equation (26) (29b)

At $i = I$:

continuity equation ($i = I-1$ in Eq. 25)
boundary condition (27b)
fluid energy equation (25)
solid energy equation (26). (29c)

The conventional method for solving Eq. (1) with an implicit scheme is to use central spatial differences and to use the transient solution to obtain the steady-state result. When this approach is applied to governing equations (1) with linearization (24), the difference equations are of the form of Eq. (28), where the *central difference* coefficients are

$$
\begin{aligned}
A_i &= \Theta\tilde{A}_{i-1}/x_T, \\
B_i &= \bar{I}/\Delta t - \Theta\tilde{D}_i, \\
C_i &= -\Theta\tilde{A}_{i+1}/x_T, \\
D_i &= S_i^n - (F_{i+1} - F_{i-1})^n/x_T, \\
x_T &= x_{i+1} - x_{i-1}, \qquad i = 2, 3, \ldots, I-1,
\end{aligned} \tag{30}
$$

$\theta = 1$, Fully implicit (or steady state solution),

$= \frac{1}{2}$, Trapezoidal scheme,

$\bar{I}$ = Unit matrix (zero for steady-state equation).

These difference equations can be used to replace midpoint difference equations (25), except that the relations for $i = 1$ have been lost. Therefore, there is a need to provide a boundary approximation at $i = 1$ and two boundary approximations at $i = I$. The solid energy equation still can be applied at $i = 1$ and I. The foregoing central difference equations (30) for the steady state can be obtained from Eqs. (23) and (25) with i replaced with $i - 1$. These two equations are added and divided by x_T to obtain the *additive midpoint* coefficients.

$$
\begin{aligned}
A_i &= (\tilde{A}_{i-1} + \tfrac{1}{2}\Delta x_{i-1}\tilde{D}_{i-1})/x_T, \\
B_i &= -\tfrac{1}{2}\tilde{D}_i, \\
C_i &= -(\tilde{A}_{i+1} - \tfrac{1}{2}\Delta x_i\tilde{D}_{i+1})/x_T, \\
D_i &= \tfrac{1}{2}[\Delta x_i(S_{i+1} + S_i)^n + \Delta x_{i-1}(S_i + S_{i-1})^n]/x_T - (F_{i+1} - F_{i-1})^n/x_T,
\end{aligned} \tag{31}
$$

for $i = 2, 3, \ldots, I-1$. The steady state form of Eqs. (30) becomes eqs. (31) if the quantities $D_i\Delta Q_i$ and S_i are evaluated with the weighting relation

$$
W_i = [\Delta x_i(W_{i+1} + W_i) + \Delta x_{i-1}(W_i + W_{i-1})]/(2x_T). \tag{32}
$$

Since difference equations (28) with additive midpoint coefficients (31) are just another formulation of the midpoint scheme, the appropriate relations at $i = 1$ and I are midpoint relations (29a) and (29c), respectively. These same boundary approximations are used with central difference scheme (30) replacing Eq. (29b).

The numerical results are obtained for the following conditions:

(i) $\varepsilon = 0.32$,

(ii) $d_p = 5 \times 10^{-6}$ m,

(iii) $\gamma = 1.4$,

(iv) $p_{in} = 1.01325 \times 10^7$ N/m^2,

(v) $p_{out} = 1.01325 \times 10^5$ N/m^2,

(vi) $T_{in} = 297.15$ K,

(vii) $L = 1$ cm,

(viii) $\mu = 1.458 \times 10^{-6} T_f^{1.5}/(T_f + 110.4)$ kg/m–s,

(ix) $h = 18.75$ J/m^2–s–K,

(x) $c_s = 880.0$ J/kg–K,

(xi) $\rho_s = 2648.0$ kg/m^3,

(xii) $\bar{M} = 28.966$ kg/(kg mol),

(xiii) $R = 8314.3$ J/(kg mol)(K).

Conditions (ix)–(xiii) are not needed for the steady-state solution. The numerical solution of the steady state form of the governing equations is readily obtained with midpoint scheme (29) and this procedure requires several iterations with rapid convergence. When central difference scheme (30) with $\theta = 1$ and $I = 0$ is used, the solution does not converge. This same behavior is observed with the additive midpoint scheme. If a subtractive midpoint scheme is developed from Eq. (25), then this approach has the same convergence properties of the midpoint scheme. In order to obtain the steady-state solution with the central difference scheme, the transient solution approach is used. With a fully implicit scheme ($\theta = 1$), a steady-state solution is obtained while with the Crank–Nicolson approach ($\theta = 0.5$), the solution tends to have small oscillations. When the transient midpoint scheme (also known as the box scheme) is used, the fully implicit scheme ($\theta = 1$) converges to a steady state while with $\theta = 0.5$, the solution has large oscillations. With more time steps the magnitude of the oscillations can be reduced. The numerical results presented with the transient procedure are for the case $\theta = 1$.

With the midpoint scheme the numerical solution is obtained without any boundary approximations. The mass flux $\rho u \varepsilon$, which is constant through the porous media, is used to judge the accuracy of the numerical solutions with the exact solution obtained with Richardson extrapolation. The accuracy of the midpoint scheme is illustrated in Fig. 4, where the number of grid points through the porous media is varied. This method has the expected second-order behavior. The accuracy of the central difference scheme with the second-order midpoint boundary approximations defined by Eqs. (29a) and 29b) has nearly the same accuracy as the midpoint scheme as shown in Fig. 4. The influence of boundary approximations with the central difference scheme is investigated by replacing momentum equation (29a) at the entry with the following first-order difference relations for the momentum equation:

$$\text{relation 1:} \quad (F_{i+1} - F_i)/\Delta x_i = S_i, \qquad i = 1, \tag{33a}$$

$$\text{relation 2:} \quad (F_{i+1} - F_i)/\Delta x_i = S_{i+1}, \qquad i = 1, \tag{33b}$$

The first boundary approximation (33a) actually improves the accuracy of the results but the overall accuracy is not completely second-order for the grid size investigated.

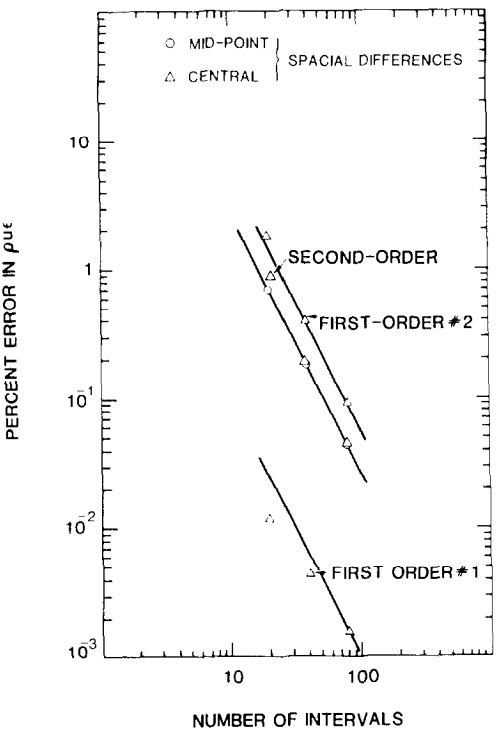

FIG. 4. Accuracy of mass flux in porous media with several entry boundary approximations.

The second boundary approximation (33b) is less accurate but the overall accuracy of the scheme has second-order behavior. The use of a first-order boundary approximation of the governing equation with a second-order interior difference scheme still results in a scheme with overall second-order behavior.

DISSIPATIVE MODEL PROBLEM

The importance of boundary condition discretization and boundary or extraneous approximations on the finite-difference solution of a dissipative type differential equation is investigated by considering the model problem

$$\frac{\partial}{\partial \eta}\left(l\frac{\partial W}{\partial \eta}\right) - b^2 W = 0 \tag{34}$$

with boundary conditions

At $\eta = 0$:

$$\text{Dirichlet} \qquad W_B = 0 \tag{35a}$$

or

$$\text{Neumann} \qquad (\partial W/\partial \eta)_B = 0 \tag{35b}$$

At $\eta = 1$:

$$W = 1 \tag{36}$$

The exact solution of this equation is

$$W_E = (e^{\alpha\eta} \pm e^{-\alpha\eta})/(e^{\alpha} \pm e^{-\alpha}), \tag{37}$$

where the plus sign corresponds to the Neumann boundary condition while the negative is for the Dirichlet boundary condition. The parameter $\alpha = b/\sqrt{l}$ and for the numerical solutions $b = l = 2$. For the Dirichlet problem, the value of W at $\eta = 0.1$ is 0.073327303 and is used to test the accuracy of the numerical solutions. For the Neumann problem, the value of W at $\eta = 0$ is 0.45909813 and is used for judging the accuracy of these numerical solutions. These exact solutions for the two types of boundary conditions are given in Fig. 5.

The numerical discretization of the boundary conditions is approximated with the following relations, where h is the grid size and the local truncation is indicated:

Dirichlet: (Boundary $\eta = 0$ is located between first and second grid points and the distance from first grid point is fh where $0 \leqslant f \leqslant 1$)

first order:

$$W_1 = W_B + O(h). \tag{38a}$$

second order:

$$W_1 = W_B - f(W_2 - W_1) + O(h^2). \tag{38b}$$

Neumann: (Boundary $\eta = 0$ at first grid point):

$$\text{first order:} \qquad (W_2 - W_1)/h = \left(\frac{\partial W}{\partial \eta}\right)_B + O(h). \tag{39a}$$

Neumann: (Boundary midway between first and second grid points):

$$\text{second order:} \qquad (W_2 - W_1)/h = (\partial W/\partial \eta)_B + O(h^2). \tag{39b}$$

The numerical solutions are obtained with a uniform grid in order to isolate the influence of the boundary condition discretization errors. The derivative in Eq. (34) is evaluated with a central difference scheme and the equation becomes

$$(W_{j+1} - 2W_j + W_{j-1})/h^2 - \alpha^2 W_j = 0, \tag{40}$$

which has a local truncation error of $O(h^2)$. The resulting difference equations and boundary conditions (38) or (39) are tri-diagonal equations of the form of Eq. (28).

With the Dirichlet boundary condition $W=0$ at $\eta=0$, the numerical solution has been obtained to the model difference equation with the boundary located midway between the first and second grid points. The results for first-order boundary [illegible] comparison of the first-order solution with the exact solution is given in Fig. 5. For this problem the first-order boundary condition approximation has a significant adverse influence on the solution which has first-order behavior.

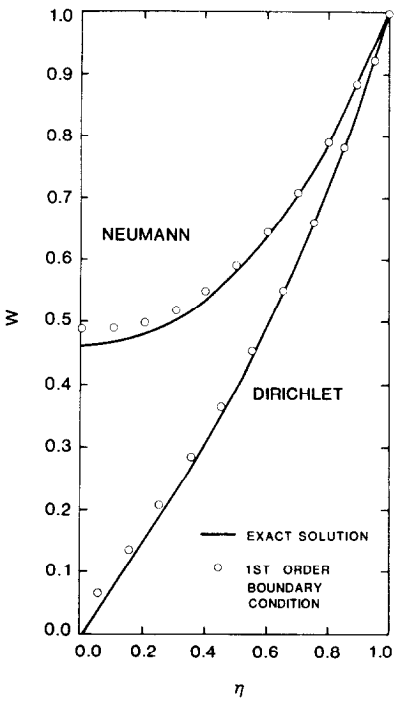

FIG. 5. Solution of dissipative model problem.

The model problem has been solved with Neumann boundary conditions with a uniform grid. The results of this study are given in Fig. 7 for the first-order boundary conditions (Eqs. (39a)) and the second-order boundary condition (Eq. (39b)). A comparison of the first-order solution with the exact solution is given in Fig. 5. With the boundary at the first grid point, a second-order boundary condition can be obtained with the use of the governing equation. A grid point $j = 0$ is introduced beyond the boundary such that $\eta_2 - \eta_1 = \eta_1 - \eta_0 = h$. The derivative boundary condition is written as

$$(W_2 - W_0)/2h = (\partial W/\partial \eta)_B + O(h^2).$$

Governing difference equation (28) is applied at the boundary and for this case becomes

$$-\bar{A}_1 W_0 + \bar{B}_1 W_1 - \bar{C}_1 W_2 = \bar{D}_1,$$

where bars have been added to the coefficients. The above equations are combined to eliminate W_0 and the boundary condition is of the form of the first equation of (28), where

$$B_1 = \bar{B}_1, \qquad C_1 = \bar{C}_1 + \bar{A}_1, \qquad D_1 = \bar{D}_1 - 2h\bar{A}_1(\partial W/\partial \eta)_B.$$

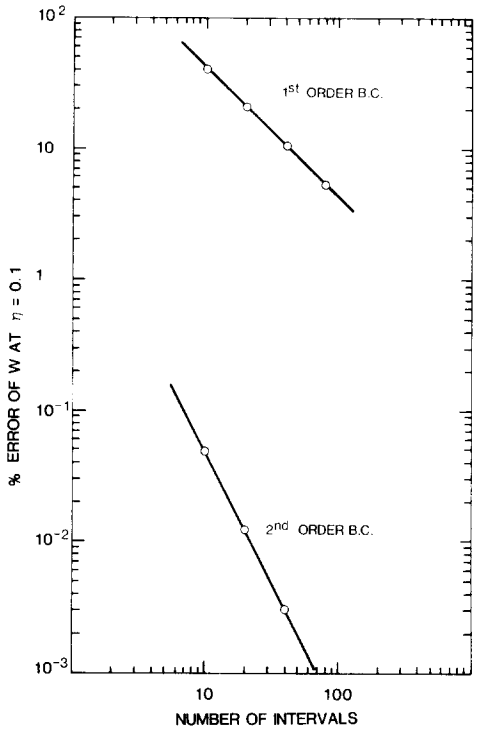

FIG. 6. Dirichlet boundary condition for dissipative model problem.

This method gives a second-order boundary condition with the same accuracy of the previous methods.

The foregoing investigation of the influence of boundary condition numerical error can also be investigated analytically. The exact solution of difference equation (40) is

$$W_j = a\sigma_1^{j-1} + b\sigma_2^{j-1} \tag{41}$$

and for the exact Dirichlet boundary condition (35a) becomes

$$W_j = (\sigma_1^{j-1} - \sigma_2^{j-1})/(\sigma_1^{J-1} - \sigma_2^{J-1}), \qquad j = 1, 2, \ldots, J, \tag{42}$$

where

$$\sigma_{1,2} = 1 \pm \alpha h + \tfrac{1}{2}(\alpha h)^2 \pm \tfrac{1}{8}(\alpha h)^3 + \cdots = e^{\pm \alpha h} \mp \tfrac{1}{24}(\alpha h)^3 + \cdots .$$

The terms in Eq. (42) are approximated as

$$\sigma_{1,2}^{j-1} = e^{\pm \alpha \eta_j}(1 \mp \tfrac{1}{24}\alpha^3 h^2 \eta_j + \cdots). \tag{43}$$

The error of the difference solution is defined as

$$E = (W_j - W_E)/W_E . \tag{44}$$

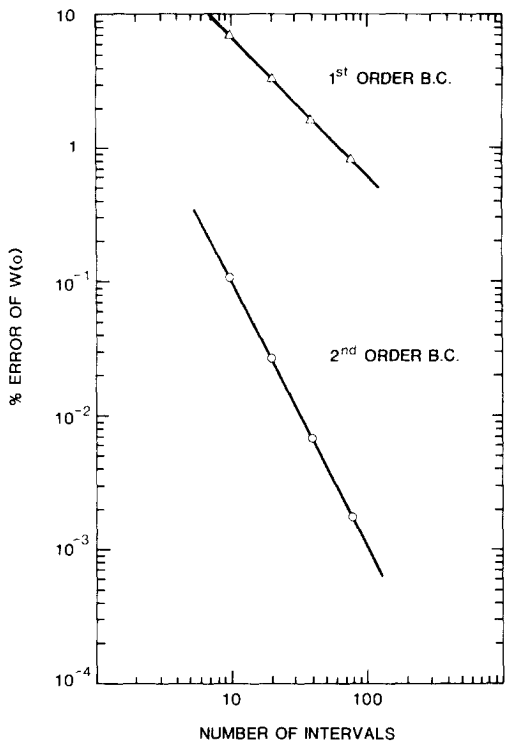

FIG. 7. Neumann boundary condition for dissipative model problem.

The difference solution or global error with the use of Eqs. (37), (42), and (43) in Eq. (44) becomes

$$E = E_2 h^2 + \cdots, \tag{45}$$

where $E_2 = \frac{1}{24}\alpha^3(\coth \alpha - \eta_j \coth \alpha\eta_j)$. This shows that the central difference scheme with exact Dirichlet boundary conditions results in a second-order global error.

Consider the case where the Dirichlet boundary condition is located between the first and second grid points. The exact solution (37) to this case is

$$W_E = \sinh \alpha\eta / \sinh \alpha. \tag{46}$$

The difference solution of Eq. (40) with boundary conditions (38) becomes

$$W_j = \phi_j / \phi_J \tag{47}$$

where $\phi_j = (1 - c\sigma_1)\,\sigma_2^{j-1} - (1 - c\sigma_2)\,\sigma_1^{j-1}$,

$$W_1 = cW_2, \qquad c = 0, \quad \text{for boundary condition (38a)},$$
$$= -f/(1-f), \quad \text{for boundary condition (38b)}.$$

Since $\eta_j = h(j-1) - f\bar{h}$ and $\sigma_{1,2}$ is given by Eq. (42), the following is obtained:

$$\sigma_{1,2}^{j-1} = e^{\pm \alpha \eta_j}\left[1 \pm f\alpha h + \tfrac{1}{2}(\alpha f\bar{h})^2 \mp \tfrac{1}{24}\alpha^3 \eta_j h^2 + \cdots\right]. \tag{48}$$

The error as defined by Eq. (44) becomes with Eqs. (37), (47), and (48):

First-order boundary condition (38a)

$$E = f\alpha(\coth \alpha\eta_j - \coth \alpha)\, h + \cdots. \tag{49a}$$

Second-order boundary condition (38b)

$$E = E_2 h^2 + \cdots. \tag{49b}$$

Therefore the global accuracy corresponds to the local truncation error of the boundary condition. The errors predicted from Eqs. (49) are the solid lines in Fig. 6 and are in excellent agreement with the numerical computations indicated with the circles.

If first-order Neumann boundary condition (39a) is used, the difference solution is

$$W_j = \phi_j/\phi_J, \tag{50}$$

where

$$\phi_j = \lambda_2 \sigma_1^{j-1} - \lambda_1 \sigma_2^{j-1},$$
$$\lambda_{1,2} = (1 - \sigma_{1,2}) = \mp \alpha h(1 \pm \tfrac{1}{2}\alpha h + \cdots).$$

With the use of Eqs. (37) and (43), the error for the above difference equation becomes:

First-order boundary condition (39a)

$$E = \tfrac{1}{2}\alpha(\tanh \alpha - \tanh \alpha\eta_j)\, h + \cdots. \tag{51a}$$

For second-order Neumann boundary condition (39b), the difference solution is given by Eq. (47), where $c = 1$. The use of Eqs. (42) and (48) with $f = 0.5$ gives the error of the difference solution as:

Second-order boundary condition (39b)

$$E = \tfrac{1}{24}\alpha^3(\tanh \alpha - \eta_j \tanh \alpha\eta_j)\, h^2 + \cdots. \tag{51b}$$

The global accuracy corresponds to the local truncation error of the Neumann boundary conditions. The errors predicted from Eqs. (51) are the solid lines in Fig. 7 and are in excellent agreement with the numerical computations indicated with the circles.

In order to investigate the influence of boundary or extraneous approximations, it is assumed that a relation is needed to determine W_2, while W_1 is known from Dirichlet boundary condition (35a). Extrapolation approximations are considered

first where the local truncation error is indicated and obtained from a Taylor's series expansion

$$\text{first order:} \qquad W_2 = W_1 + O(h), \tag{52a}$$

$$\text{second order:} \qquad W_2 = W_1 + \tfrac{1}{2}(W_3 - W_1) + O(h^2). \tag{52b}$$

The finite-difference solution is given by Eq. (50), where

$$\lambda_{1,2} = \sigma_{1,2} = 1 \pm \alpha h + \cdots \tag{53a}$$

and

$$\lambda_{1,2} = \sigma_{1,2}(\sigma_{1,2} - 2) = -1 + (\alpha h)^2 \pm (\alpha h)^3 + \cdots \tag{53b}$$

for the first- and second-order approximations, respectively. The solution error becomes:

First-order boundary approximation (52a)

$$E = \alpha(\coth \alpha - \coth \alpha\eta_j)\, h + \cdots . \tag{54a}$$

Second-order boundary approximation (52b)

$$E = E_2 h^2 + \cdots . \tag{54b}$$

The locally second-order extrapolation approximation results in global second-order accuracy and has the same error as central difference scheme (45).

Another approach for obtaining a boundary approximation is to difference the governing equation; for this case the result is

$$(W_{j+1} - 2W_j + W_{j-1})/h^2 - \alpha^2[\Theta W_{j-1} + (1 - \Theta)\, W_j] = 0, \tag{55}$$

where

$\Theta = 1$, first-order local truncation error,

$= 0$, second-order local truncation error.

If $\Theta = 0$, then Eq. (40) is obtained and a second-order global accuracy results as given by Eq. (45). If $\Theta = 1$, the solution to difference equation (55) is given by Eq. (42), where

$$\sigma_{1,2} = 1 \pm \alpha h \qquad \text{and} \qquad \sigma_{1,2}^{j-1} = e^{\pm \alpha \eta_j}(1 - \tfrac{1}{2}\alpha^2 \eta_j h + \cdots).$$

The difference solution error becomes

$$E = \tfrac{1}{2}\alpha^2(1 - \eta_j)\, h + \cdots ,$$

which shows that the global accuracy is first-order. If the first-order form of Eq. (55) is used at $j = 2$, difference relation (55) becomes

$$W_2 = \tfrac{1}{2}[(W_1 + W_3) - (\alpha h)^2\, W_1] + O(h^3). \tag{56}$$

When this approximation is used along with the second-order form of Eq. (55) at all the remaining grid points, the difference solution error is the same as Eq. (45) and the global error is second-order. This behavior has been observed previously by Srivastava, Werle, and Davis [14] and is the only case where a first-order approximation has not destroyed the second-order global accuracy. Although Eq. (56) represents the governing equation with a first-order local truncation error, the approximation appears to be third-order when written as Eq. (56) and compared to extrapolation relations (52). This example illustrates the importance of stating whether extrapolation or a difference form of the governing equation is being used to provide the boundary approximation.

Summary of Results

(1) For the quasi-one-dimensional flow in a duct with the interior grid points solved with the MacCormack scheme, the boundary approximations have the following influences on the accuracy of the solution:

(a) For boundary approximation difference relations that are inconsistent with the interior scheme, small oscillations near the boundary occur.

(b) The midpoint relation gives the most accurate results for the procedures investigated.

(c) With first-order extrapolation boundary approximations, the global accuracy is generally reduced to first order.

(2) An interior implicit midpoint difference technique is utilized for solving the compressible one-dimensional flow in a porous material (or quasi-one-dimensional flow with friction). This procedure is consistent with the boundary conditions and does not require any boundary approximations. When spatial central differences are used in the interior implicit scheme, three boundary approximations are required to complete the system of difference equations. The midpoint scheme provides guidance in indicating the appropriate boundary approximations to be employed. If first-order boundary approximations to the governing equations are used, the global accuracy of the solutions still tends to be second order. The extension of the midpoint rule to time dependent problems with two space dimensions is not readily performed and requires development. The author [15] has used this concept for solving the inviscid supersonic two-dimensional flow over a pointed ogive where a marching procedure is used along the body.

(3) Boundary condition discretization accuracy has significant influence on the global accuracy of a dissipative (second derivative) model problem. When a second-order interior difference scheme is used, the use of first-order boundary condition discretization reduces the overall accuracy of the solution to first order. This result occurs for both Dirichlet and Neumann boundary conditions. A boundary approximation investigation indicates that global second-order accuracy is retained with

second-order extrapolation and with the model equation approximated with first-order accuracy.

The results of the problems investigated indicate that first-order boundary approximations derived from the governing equations give second-order global accuracy while first-order boundary approximations resulting from extrapolation give first-order global accuracy. For boundary condition discretization, first-order difference relations result in first-order global accuracy while second-order difference relations are required to retain second-order behavior.

REFERENCES

1. E. TURKEL, *in* "Computational Fluid Dynamics," Vol. 2 (W. Kollmann, Ed.), McGraw–Hill (Hemisphere), New York, 1980.
2. B. GUSTAFSSON, *Math. Comp.* **29** (1975), 396.
3. G. SKOLLERMO, *Math. Comp.* **33** (1979), 11.
4. J. H. BRAMBLE AND B. E. HUBBARD, *Numer. Math.* **4** (1962), 313.
5. P. D. THOMAS, AIAA Computational Fluid Dynamics Conference, Paper No. 79-1447, 1979.
6. G. MORETTI AND M. PANDOLFI, *AIAA J.* **19** (1981), 449.
7. A. H. SHAPIRO, "Compressible Fluid Flow," Vol. II, Ronald Press, New York, 1954.
8. M. D. GRIFFIN AND J. D. ANDERSON, JR., *Comput. and Fluids*, **5** (1977), 127.
9. S. ERGUN, *Chem. Engrg. Prog.* **48** (1952), 89.
10. G. EMANUEL AND J. P. JONES, *Internat. J. Heat Mass Transfer* **11** (1968), 827.
11. T. E. W. SCHUMANN, *J. Franklin Inst.* **208** (1929), 405.
12. F. A. MORRISON, *Trans. ASME, J. Fluids Engrg.*, **99** (1977), 779.
13. S. V. PATANKAR, "Numerical Heat Transfer and Fluid Flow," McGraw–Hill (Hemisphere), New York, 1980.
14. B. N. SRIVASTAVA, M. J. WERLE, AND R. T. DAVIS, *Comput. and Fluids* **7** (1979), 69.
15. F. G. BLOTTNER, "Exact and Approximate Solutions of the Inviscid Shock Layer Flow With an Implicit Finite-Difference Scheme," Sandia Laboratories Report SAND78-0896, Albuquerque New Mexico, June 1978.